Unique Fluxional Behavior. Synthesis, Structure, and Properties of Novel (Diamine)platinum(II) Complexes of 9-Fluorenylidene- and Benzhydrylidenemalonate Ligands

Young-A Lee,[†] Ok-Sang Jung,[†] Seong-Joo Kang,[†] Kang-Bong Lee,[‡] and Youn Soo Sohn*[,†]

Inorganic Chemistry Laboratory and Advanced Analysis Center, Korea Institute of Science and Technology, Seoul 130-650, Korea

Received August 3, 1995[⊗]

New (diamine)platinum(II) complexes A_2PtX_2 (A_2 = *trans*-(±)-1,2-diaminocyclohexane (DACH), tetrahydro-4*H*-pyran-4,4-diylbis(methylamine)(THPDMA); X_2 = 9-fluorenylidenemalonate(FM), benzhydrylidenemalonate-(BHM)) have been synthesized and characterized by means of multinuclear NMR spectroscopy and X-ray analysis. (DACH)Pt(FM) crystallizes in space group $P2_1/c$ with eight formula units in a cell of dimensions $a = 20.071(7)$ Å, $b = 12.717(3)$ Å, $c = 24.512(6)$ Å, $\beta = 103.25(2)°$, and $V = 6090(3)$ Å.^{3} (DACH)Pt(BHM) crystallizes in space group $P\bar{1}$ with four molecular units in a cell of dimensions $a = 11.048(3)$ Å, $b = 13.639(3)$ Å, $c = 14.043(6)$ Å, $\alpha = 90.17(3)°$, $\beta = 91.31(4)°$, $\gamma = 89.98(3)°$, and $V = 2116(1)$ Å^3. The platinum atom in both complexes adopts a typical square planar arrangement with two nitrogen atoms in *cis* position. The 9-fluorenylidene and benzhydrylidene groups of the amine ligands chelated to platinum are strikingly bent up by 88.8(3) and 80.8(2)°, respectively, from the platinum square plane in the solid state. Variable temperature ^{1}H NMR spectra of the title complexes in dimethyl sulfoxide solution reveals that the amine proton resonances are sensitive to the fluxional motion of the remote arylidene groups, and suggests that interconversion occurs between two "bent-up" and "bent-down" forms. The prominent difference between the FM and BHM complexes is observed in solution, due to the presence or absence of the angle constraint of the anionic coligands.

Introduction

Many platinum complexes bearing potent antitumor activity are composed of bioactive *cis*-(diamine)platinum(II) fragments and various dicarboxylate ligands.[1−4] Among the complexes, only *cis*-diammine(1,1-cyclobutanedicarboxylato)platinum(II) (carboplatin) was clinically approved as a second generation platinum anticancer drug. It does not exhibit significant nephrotoxicity and emesis compared with cisplatin.[5,6] The nephrotoxicity of cisplatin has been known to be associated with its active hydrolysis products, which form over a period of minutes,[7] whereas the relatively lower toxicities of carboplatin were found to be related to its pharmacokinetic stability in solution.[8] Accordingly, the platinum complexes of various dicarboxylate ligands have been screened for more effective anticancer drugs with less toxicities.[9−12] As a consequence, several platinum complexes of carboxylate ligands have entered clinical trials for new generation platinum anticancer agents.[13−16] Thus, the structure and behavior of the anionic carboxylate ligands play an important role in determining the pharmacokinetic stability of their platinum complexes.

In this paper, (diamine)platinum(II) complexes of structurally interesting dicarboxylate ligands, 9-fluorenylidenemalonate (FM)and benzhydrylidenemalonate (BHM), have been synthesized, and their dynamic structural behaviors in solution are reported based on their multinuclear NMR spectra along with the X-ray crystal structures of the FM and BHM complexes. As carrier ligand *trans*-(±)-1,2-diaminocyclohexane (DACH) and tetrahydro-4H-pyran-4,4-diylbis(methylamine) (THPDMA) were used since not only do they form stable platinum

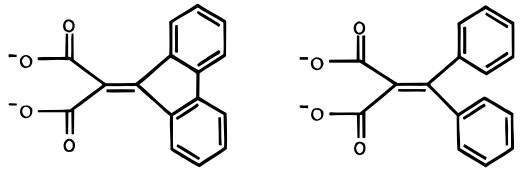

FM BHM

[†] Inorganic Chemistry Laboratory, Korea Institute of Science and Technology.

[‡] Advanced Analysis Center, Korea Institute of Science and Technology.

[⊗] Abstract published in *Advance ACS Abstracts,* February 15, 1996.

(1) Brunner, H.; Obermeier, H. *Angew. Chem., Int. Ed. Engl.* **1994**, *33*, 2214.
(2) Appleton, T. G.; Hall, J. R.; Neale, D. W.; Thompson, C. S. M. *Inorg. Chem.* **1990**, *29*, 3985.
(3) Talebian, A. H.; Bensely, D.; Ghioghis, A.; Hammern, C. F.; Schein, P. S.; Green, D. *Inorg. Chim. Acta* **1991**, *179*, 281.
(4) Gibson, D.; Rosenfeld, A.; Apfelbaum, H.; Blum, J. *Inorg. Chem.* **1990**, *29*, 5125.
(5) Harland, S. J.; Newell, D. R.; Siddik, J. H.; Chadwick, R.; Calvert, A. H.; Harrap, K. R. *Cancer Res.* **1984**, *44*, 1693.
(6) Mauldin, S. K.; Husain, I.; Sancar, A.; Chaney, S. G. *Cancer Res.* **1986**, *46*, 2876.
(7) Cleare, M. J.; Hydes, P. C.; Malerbi, B. W.; Watkins, D. M. *Biochimie* **1978**, *60*, 835.
(8) Van der Vijgh, W. J. F. *Clin. Pharmacokinet.* **1991**, *21*, 242.
(9) Pasini, A. *Inorg. Chim. Acta* **1987**, *137*, 57.
(10) Barnard, C. F. J.; Cleare, M. J.; Hydes, P. C. *Chem. Br.* **1986**, 1001.
(11) Sherman, S. E.; Lippard, S. J. *Chem. Rev.* **1987**, *87*, 1153.
(12) Van Kralingen, C. G.; Reedijk, J.; Spek, A. L. *Inorg. Chem.* **1980**, *19*, 1481.
(13) Weiss, R. B.; Christian, M. C. *Drugs* **1993**, *46*, 360.
(14) (a) Bitha, P.; Carvajal, S. G.; Citarella, R. V.; Child, R. G.; Delos Santos, E. F.; Dunne, T. S.; Durr, F. E.; Halavaka, J. J.; Lang, S. A., Jr.; Lindsay, H. L.; Morton, G. O.; Thomas, T. S.; Wallace, R. E.; Lin, Y.-I.; Haltiwanger, R. C.; Pierpont, C. G. *J. Med. Chem.* **1989**, *32*, 2015. (b) Al-Baker, S.; Siddiq, Z. H.; Khokhar, A. R. *J. Coord. Chem.* **1994**, *31*, 109.
(15) Harstrick, A.; Bokemeyer, C.; Scharnofkse, M.; Hapke, G.; Reile, D.; Schmoll, H.-J. *Cancer Chemo. Pharm.* **1993**, *33*, 43.
(16) Yonei, T.; Ohnoshi, T.; Hiraki, S.; Ueoka, H.; Kiura, K.; Moritaka, T.; Shibayama, T.; Tabata, M.; Segawa, Y.; Takigawa, N.; Kimura, I. *Acta Med. Okayama* **1993**, *47*, 233.

0020-1669/96/1335-1641$12.00/0

complexes, but also their platinum complexes exhibit high antitumor activity with no cross-resistance to cisplatin.[14]

Experimental Section

Instrumentation. Elemental analyses were performed by the Advanced Analysis Center at KIST. The infrared spectra in the 5000−400 cm^{-1} region were measured as KBr pellets on a Perkin Elmer 16F PC model FT-IR spectrometer. ^1H, ^{13}C, and ^{195}Pt NMR spectra were recorded on a Varian Gemini-300 NMR spectrometer operating at 300.00 MHz (^1H), 75.48 MHz (^{13}C) and 64.39 MHz (^{195}Pt) in pulse mode with Fourier transform. Variable temperature ^1H NMR spectra were measured on a Varian Unity *Plus* 600 MHz NMR spectrometer. The chemical shifts were relative to $SiMe_4$ (^1H and ^{13}C) and Na_2PtCl_6 (^{195}Pt) as an internal or external standard for the indicated nuclei. The mass analysis was achieved on a platform (Fisons Inst., Manchester, U.K.) equipped with an electrospray source at 10 L/min using a Havard infusion pump. For the mass analysis, appropriate amount of samples were dissolved in a solvent mixture of MeOH and water (50:50,V/V) containing 1% acetic acid.

Materials. Potassium tetrachloroplatinate(II)(Kojima) and DACH (Aldrich) were used as received. THPDMA was prepared according to the literature.[14] The FM and BHM ligands were prepared by literature procedures[17] and converted to barium salts, which were reacted with (diamine)platinum sulfate.[18] *cis*-(Diamine)platinum(II) sulfates were also prepared by the literature method.[19,20]

Synthesis of (DACH)Pt(FM). To a suspension of (DACH)-$PtSO_4 \cdot H_2O$ (0.42 g, 1.0 mmol) in water (50 mL) was added $Ba(FM)_2 \cdot 2H_2O$ (0.44 g, 1.0 mmol) in methanol (50 mL). The reaction mixture was stirred for 3 h. After barium sulfate was filtered off, the filtrate was evaporated to dryness to obtain a yellow solid in 78.1% yield. Slow evaporation of its DMF solution gave crystals suitable for X-ray crystallography: mp 219 °C dec. Anal. Calcd for $C_{22}H_{22}N_2O_4Pt$: C, 46.07; H, 3.87; N, 4.88. Found: C, 45.80; H, 3.94; N, 4.81. ^1H NMR (Me_2SO-d_6, ppm): δ = 0.91 (s, 2H); 1.13 (s, 2H); 1.38 (d, 2H, 9.15 Hz); 1.74 (d, 2H, J = 11.37 Hz); 1.92 (s, 1H); 2.04 (s, 1H); 5.21 (s, NH, 1H); 5.50 (s, NH, 1H); 5.87 (s, NH, 1H); 6.10 (s, NH, 1H); 7.25 (t, 2H, J = 7.68/7.41 Hz); 7.38 (t, 2H, J = 7.32 Hz); 7.85 (d, 2H, J = 7.32 Hz); 8.04 (d, 2H, J = 7.47 Hz). ^{13}C NMR (Me_2SO-d_6, ppm): 24.0, 31.2, 62.1, 119.4, 125.3, 125.6, 127.1, 128.3, 136.9 (C═C), 139.4 (C═C), 171.7 (C═O). ^{195}Pt NMR (Me_2SO-d_6, ppm); −1844. IR (KBr, cm^{-1}): $\nu(COO)_{asym}$, 1648, 1592; $\nu(COO)_{sym}$, 1322. Mass: m/e = 574.0 $[M + H]^+$, 530.1 $[M + H - CO_2]^+$, 486.1 $[M + H - 2CO_2]^+$.

Synthesis of (DACH)Pt(BHM). This compound was prepared in 75.7% yield by the same procedure used for (DACH)Pt(FM) with BHM used instead of FM: mp 202 °C dec. Slow evaporation of its methanol solution gave crystals suitable for X-ray crystallography. Anal. Calcd for $C_{22}H_{24}N_2O_4Pt \cdot H_2O$: C, 44.52; H, 4.42; N, 4.72. Found: C, 44.30; H, 4.51; N, 4.49. ^1H NMR (Me_2SO-d_6, ppm): δ = 0.98−1.08 (m, 2H); 1.20−1.36 (m, 2H); 1.42−1.51 (m, 2H); 1.85 (d, 2H, J = 37 Hz); 2.08−2.19 (m, 2H); 5.33 (t, NH_2, 2H, J = 7.20 Hz); 6.05 (d, NH_2, 2H, J = 8.07 Hz); 7.19−7.30 (m, 6H); 7.33−7.41 (m, 4H). ^{13}C NMR (Me_2SO-d_6, ppm): 24.0, 31.3, 62.1, 126.7, 127.3, 129.2, 135.4, 140.0 (C═C), 141.4 (C═C), 171.7 (C═O). ^{195}Pt NMR (Me_2SO-d_6, ppm): −1873. IR (KBr, cm^{-1}): $\nu(COO)_{asym}$, 1636, 1613; $\nu(COO)_{sym}$, 1342. Mass: m/e = 576.2 $[M + H]^+$, 532.1 $[M + H - CO_2]^+$, 488.1 $[M + H - 2CO_2]^+$.

Synthesis of (THPDMA)Pt(FM). This compound was prepared in 80.1% yield by the same procedure used for (DACH)Pt(FM) with THPDMA used instead of DACH: mp 194 °C dec. Anal. Calcd for $C_{23}H_{24}N_2O_5Pt$: C, 45.77; H, 4.01; N, 4.64. Found: C, 44.90; H, 3.89; N, 4.69. ^1H NMR (Me_2SO-d_6, ppm): δ = 1.25 (s, 4H); 2.17 (s, 4H); 3.39 (s, 4H); 5.23 (s, NH_2, 2H); 5.72 (s, NH_2, 2H); 7.24 (t, 2H, J = 7.50/7.62 Hz); 7.38 (t, 2H, J = 7.41/7.29 Hz); 7.84 (d, 2H, J = 7.35 Hz); 8.03 (d, 2H, J = 7.68 Hz). ^{13}C NMR (Me_2SO-d_6, ppm): 31.1, 34.5, 49.9, 62.0, 119.4, 125.2, 125.8, 127.0, 128.3, 136.8, 138.9 (C═C), 139.4 (C═C), 171.7 (C═O). ^{195}Pt NMR (Me_2SO-d_6, ppm): −1884. IR (KBr, cm^{-1}): $\nu(COO)_{asym}$, 1652, 1628; $\nu(COO)_{sym}$, 1322. Mass: m/e = 604.2 $[M + H]^+$, 560.1 $[M + H - CO_2]^+$, 516.1 $[M + H - 2CO_2]^+$.

Table 1. Crystallographic Data for (DACH)Pt(FM) and (DACH)Pt(BHM)

	(DACH)Pt(FM)	(DACH)Pt(BHM)
formula	$C_{22}H_{22}N_2O_4Pt_1 \cdot 0.9DMF \cdot 0.6H_2O$	$C_{22}H_{20}N_2O_4Pt_1 \cdot H_2O$
fw	632.08	589.51
wavelength, Å	0.71073	0.71073
space group	$P2_1/c$ (No. 14)	$P\bar{1}$ (No. 2)
a, Å	20.071(7)	11.048(3)
b, Å	12.717(3)	13.639(3)
c, Å	24.512(6)	14.043(6)
α, deg	90.0	90.17(3)
β, deg	103.25(2)	91.31(4)
γ, deg	90.0	89.98(3)
V, Å^3	6090(3)	2116(1)
Z	8	4
d_{calcd}, g/cm^3	1.377	1.851
abs coeff, mm^{-1}	4.641	6.669
no. of reflcns collcd	7946	6545
no. of indep reflcns	7694	6192
GOF on F^2	1.111	1.121
final R indices $\{I > 2\sigma(I)\}^a$	R1 = 0.0627, wR2 = 0.1598	R1 = 0.0300, wR2 = 0.0668
R indices (all data)	R1 = 0.0757, wR2 = 0.1960	R1 = 0.0325, wR2 = 0.0681
largest diff peak and hole, e Å^{-3}	+1.137 and −0.830	+1.274 and −0.747

^{a} $R1 = \sum||F_o| - |F_c||/\sum|F_o|$. $wR2 = \{\sum w(F_o^2 - F_c^2)^2/\sum wF_o^4\}^{1/2}$, where $w = 1/\{\sigma^2F_o^2 + (0.0197P)^2 + 0.00P\}$ and where $P = \{\mathrm{Max}(F_o^2,0) + 2F_c^2\}/3$.

Synthesis of (THPDMA)Pt(BHM). This compound was prepared in 74.2% yield by the same procedure used for (DACH)Pt(FM). The crude product was recrystallized in MeOH to afford a yellow crystalline solid: mp 232 °C dec. Anal. Calcd for $C_{23}H_{26}N_2O_5Pt \cdot H_2O$; C, 44.30; H, 4.53; N, 4.49. Found: C, 44.10; H, 4.51; N, 4.40. ^1H NMR (Me_2SO-d_6, ppm): δ = 1.41 (s, 4H); 2.29 (s, 4H); 3.51 (s, 4H); 5.48 (s, NH_2, 4H); 7.19−7.30 (m, 6H); 7.33−7.40 (m, 4H). ^{13}C NMR (Me_2SO-d_6, ppm): 31.1, 34.6, 50.0, 62.1, 126.7, 127.5, 129.2, 135.3, 140.0 (C═C), 141.4 (C═C), 171.8 (C═O). ^{195}Pt NMR (Me_2SO-d_6, ppm): −1917. IR (KBr, cm^{-1}): $\nu(COO)_{asym}$, 1654, 1638; $\nu(COO)_{sym}$, 1324. Mass: m/e = 602.2 $[M + H]^+$, 562.1 $[M + H - CO_2]^+$, 518.2 $[M + H - 2CO_2]^+$.

X-ray Crystal Analysis. Each crystal was wedged in a Lindemann capillary with mother liquor. The X-ray data were collected on an Enraf-Nonius CAD4 automatic diffractometer with graphite-monochromated Mo Kα (λ = 0.710 73 Å) at ambient temperature. Unit cell dimensions were based on 25 well-centered reflections by using a least-square procedure. During the data collection, three standard reflections monitored every hour did not show any significant intensity variation. The data were corrected for Lorentz and polarization effects. Absorption effects were corrected for by the empirical ψ-scan method. The structures were solved by the Patterson method (SHELXS-86) and were refined by full-matrix least-squares techniques (SHELXL-93).[21] For (DACH)Pt(FM), the light atoms of the cyclohexane group and solvent molecules were refined isotropically due to the disorder problem, and other non-hydrogen atoms, anisotropically. For (DACH)Pt(BHM), all non-hydrogen atoms were refined anisotropically and hydrogen atoms were added at calculated positions. Crystal parameters and procedural information corresponding to data collection and structure refinement are given in Table 1. Final atomic coordinates and isotropic thermal parameters of (DACH)Pt(FM) are given in Tables 2 and 3.

Results and Discussion

Synthesis. The reaction of (diamine)platinum(II) sulfate with barium salts of FM and BHM ligands in the solvent mixture of

(17) Lehnert, W. *Tetrahedron* **1973**, *29*, 635.
(18) Sohn, Y. S.; Kim, K. M. U.S. Pat. 5,142,075 (1992).
(19) Johnson, G. L. *Inorg. Synth.* **1966**, *8*, 242.
(20) Gandolfi, O.; Apfelbaum, H. C.; Blum, J. *Inorg. Chim. Acta* **1987**, *135*, 27.
(21) (a) Sheldrick, G. M. SHELXS-86; A Program for Structure Determination; University of Gottingen, Germany, 1986. (b) Sheldrick, G. M. SHELXL-93: A Program for Structure Refinement: University of Gottingen, Germany, 1993.

Table 2. Atomic Coordinates ($\times 10^4$) and Equivalent Isotropic Displacement Parameters ($Å^2 \times 10^3$) for (DACH)Pt(FM)

	x	*y*	*z*	*U*(eq)[a]	occ
Pt(1)	2229(1)	5009(1)	4378(1)	45(1)	
O(1)	2186(5)	4051(8)	3718(4)	55(3)	
O(2)	1542(5)	3134(9)	3038(5)	71(3)	
O(3)	1472(5)	4162(9)	4597(4)	56(3)	
O(4)	607(5)	3115(9)	4301(5)	68(3)	
N(1)	2348(6)	6008(11)	5050(5)	65(4)	
N(2)	3031(6)	5837(9)	4212(5)	57(3)	
C(1)	1582(8)	3727(13)	3410(6)	55(4)	
C(2)	989(7)	3771(12)	4196(6)	48(3)	
C(3)	983(7)	4128(11)	3618(5)	44(3)	
C(4)	483(7)	4734(11)	3306(6)	47(3)	
C(5)	428(7)	5134(12)	2730(6)	50(4)	
C(6)	−139(8)	5819(14)	2599(7)	63(4)	
C(7)	−290(11)	6287(18)	2091(8)	102(8)	
C(8)	106(13)	6113(21)	1690(8)	113(8)	
C(9)	673(26)	5642(43)	1829(20)	80(15)	0.50
C(9′)	575(24)	5245(38)	1771(19)	76(14)	0.50
C(10)	813(10)	4890(17)	2328(7)	85(6)	
C(11)	−109(7)	5197(12)	3499(6)	52(4)	
C(12)	−459(8)	5846(13)	3073(6)	60(4)	
C(13)	−1021(10)	6376(16)	3116(8)	92(7)	
C(14)	−1268(9)	6201(18)	3619(9)	94(7)	
C(15)	−910(9)	5660(18)	4037(8)	89(7)	
C(16)	−343(10)	5109(16)	3973(8)	85(6)	
C(17)	3070(18)	6473(27)	5136(14)	58(8)	0.50
C(17′)	2801(19)	6845(30)	4956(15)	67(9)	0.50
C(18)	3156(26)	7288(41)	5633(20)	75(16)	0.50
C(18′)	3117(24)	7368(39)	5488(20)	50(14)	0.50
C(19)	3656(23)	8232(37)	5496(18)	87(12)	0.50
C(19′)	3920(19)	7799(31)	5645(15)	68(10)	0.50
C(20)	4313(25)	7647(39)	5256(20)	102(14)	0.50
C(20′)	4040(18)	8112(29)	5098(14)	64(9)	0.50
C(21)	3895(9)	7202(15)	4638(7)	77(5)	
C(22)	3165(15)	6782(24)	4594(12)	44(7)	0.50
C(22′)	3347(16)	6335(26)	4747(13)	54(8)	0.50

[a] *U*(eq) is defined as one-third of the trace of the orthogonalized $\mathbf{U}_{ij}$ tensor.

water and methanol afforded the title complexes in high yields with precipitation of barium sulfate according to eq 1. Recrys-

$$A_2PtSO_4 + BaL_2 \xrightarrow[\text{room temp}]{H_2O/MeOH} A_2PtL_2 + BaSO_4\downarrow \qquad (1)$$

$$A_2 = \text{THPDMA, DACH; } L_2 = \text{FM, BHM}$$

tallization of the complexes in methanol resulted in white or light yellow crystalline solid products, which decompose in the range 194−232 °C. The complexes are less soluble in water than carboplatin, but more soluble in polar organic solvents such as methanol, ethanol, dimethylformamide, and Me_2SO, *etc*., presumably due to the low hydrophilicities of the anionic ligands. They are stable in aqueous and Me_2SO solutions at least for a few weeks at room temperature. The stability of the complexes in solutions seems to be ascribed to the chelation effect of both the amine and anionic ligands, which may be related to pharmacokinetic behavior.

Structures of (DACH)Pt(FM) and (DACH)Pt(BHM). For the (DACH)Pt(FM), there are two independent molecules in an asymmetric region of the monoclinic unit cell and the features of the two molecules are within error of being identical. One of the molecules and its labeling scheme for (DACH)Pt(FM) is depicted in Figure 1, and selected bond distances and angles are listed in Table 4. The local geometry around the platinum atom approximates to a square planar arrangement: distances of Pt(1)−N(1), Pt(1)−N(2), Pt(1)−O(1), and Pt(1)−O(3) are 2.05(1), 2.04(1), 2.01(1), and 2.03(1) Å, respectively, and the bond angles of N(1)−Pt(1)−N(2), N(1)−Pt(1)−O(1), N(2)−Pt(1)−O(3), and O(1)−Pt(1)−O(3) are 83.5(5), 175.7(4), 175.9(4), and 89.7(4)°, respectively, which are similar to the corresponding values of *cis*-[Pt(OXTDMA)($CH_2(CO_2)_2$)].[14] The bond lengths of C(1)−O(1) (1.34(2) Å) and C(2)−O(3) (1.31(2) Å) are longer than those of C(1)−O(2) (1.17(2) Å) and C(2)−O(4) (1.20(2) Å), being consistent with typical monodentate carboxylates in other platinum(II) complexes.[22] The most interesting feature is that the 9-fluorenylidene group of the FM ligand is strikingly bent from the platinum square plane (dihedral angle between the two planes = 88.8(3)°). Even though the FM ligand is an α,β-unsaturated carboxylic acid, the bending prevents delocalization of its π electrons. As a proof of the localization, the bond length (1.35(2) Å) of the

Table 3. Atomic Coordinates ($\times 10^4$) and Equivalent Isotropic Displacement Parameters ($Å^2 \times 10^3$) for (DACH)Pt(BHM)

	x	*y*	*z*	*U*(eq)[a]
Pt(1)	4999	1204	272	33(1)
O(12)	8570(4)	1154(3)	−385(4)	52(1)
O(11)	6767(4)	844(3)	257(3)	43(1)
O(13)	5077(4)	1592(4)	−1120(3)	50(1)
O(14)	5946(4)	2491(3)	−2204(3)	47(1)
N(11)	3200(5)	1482(4)	370(4)	49(1)
N(12)	4862(5)	833(4)	1651(4)	42(1)
C(1)	7503(5)	1376(4)	−210(4)	34(1)
C(2)	5956(5)	2132(4)	−1411(4)	34(1)
C(3)	7007(5)	2288(4)	−109(4)	30(1)
C(4)	7486(5)	3166(4)	−513(4)	32(1)
C(5)	8359(5)	3315(4)	308(4)	32(1)
C(6)	9471(6)	3749(4)	173(5)	42(2)
C(7)	10251(6)	3923(5)	941(5)	50(2)
C(8)	9911(7)	3681(5)	1839(5)	50(2)
C(9)	8812(7)	3257(5)	1991(5)	48(2)
C(10)	8021(6)	3064(4)	1215(4)	41(2)
C(11)	7130(5)	4095(4)	−1024(4)	34(1)
C(12)	6474(6)	4811(5)	−532(5)	47(2)
C(13)	6157(7)	5687(5)	−983(7)	63(2)
C(14)	6488(8)	5859(6)	−1907(7)	69(3)
C(15)	7176(7)	5179(6)	−2380(5)	60(2)
C(16)	7485(6)	4283(5)	−1939(5)	43(2)
C(17)	2771(7)	1251(7)	1304(5)	63(2)
C(18)	3666(7)	1039(8)	1999(6)	74(3)
C(19)	3365(7)	798(7)	2963(5)	65(2)
C(20)	2126(8)	1026(9)	3261(6)	94(3)
C(21)	1218(8)	1249(8)	2555(7)	92(3)
C(22)	1551(7)	1501(6)	1579(6)	64(2)

[a] *U*(eq) is defined as one-third of the trace of the orthogonalized $\mathbf{U}_{ij}$ tensor.

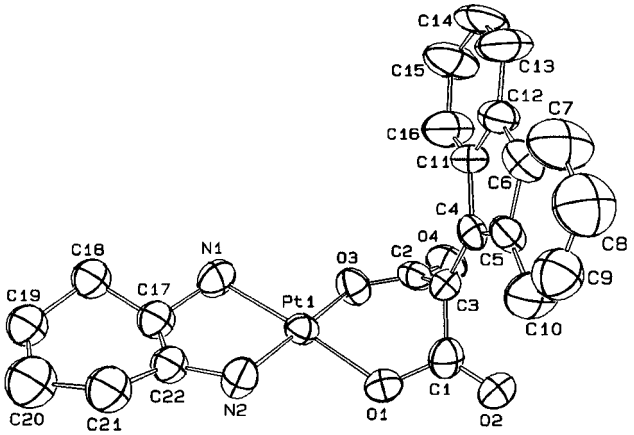

Figure 1. ORTEP drawing of (DACH)Pt(FM) showing the atom-numbering scheme. The thermal ellipsoids are drawn at the 50% probability level.

(22) Bitha, P.; Morton, G. O.; Dunne, T. S.; Delos Santos, E. F.; Lin, Y.; Boone, S. R.; Haltiwanger, R. C.; Pierpont, C. G. *Inorg. Chem.* **1990**, *29*, 645.

Table 4. Selected Bond Lengths (Å) and Angles (deg) for (DACH)Pt(FM) and (DACH)Pt(BHM)

	(DACH)Pt(FM)	(DACH)Pt(BHM)
Pt(1)−O(1)	2.011(9)	2.015(4)
Pt(1)−O(3)	2.032(10)	2.031(4)
Pt(1)−N(1)	2.050(12)	2.031(5)
Pt(1)−N(2)	2.041(11)	2.012(5)
O(1)−C(1)	1.34(2)	1.281(7)
O(2)−C(1)	1.17(2)	1.224(7)
O(3)−C(2)	1.31(2)	1.293(7)
O(4)−C(2)	1.20(2)	1.218(7)
C(1)−C(3)	1.50(2)	1.525(8)
C(2)−C(3)	1.49(2)	1.521(8)
C(3)−C(4)	1.35(2)	1.335(8)
C(4)−C(5)	1.48(2)	1.500(8)
C(4)−C(11)	1.50(2)	1.506(8)
C(5)−C(6)	1.41(2)	1.382(8)
C(5)−C(10)	1.42(2)	1.379(8)
C(6)−C(7)	1.35(2)	1.386(9)
C(7)−C(8)	1.42(3)	1.365(10)
C(8)−C(9)	1.26(5)	1.366(10)
C(9)−C(10)	1.53(5)	1.406(9)
C(6)−C(12)	1.45(2)	
O(1)−Pt(1)−O(3)	89.7(4)	89.5(2)
O(1)−Pt(1)−N(2)	92.5(4)	92.4(2)
O(1)−Pt(1)−N(1)	175.7(4)	175.4(2)
O(3)−Pt(1)−N(1)	94.2(5)	94.5(2)
O(3)−Pt(1)−N(2)	175.9(4)	178.0(2)
N(2)−Pt(1)−N(1)	83.5(5)	83.5(2)
O(1)−C(1)−C(3)	113.4(12)	118.2(5)
O(3)−C(2)−C(3)	116.2(12)	116.3(5)
C(1)−C(3)−C(2)	112.8(12)	116.5(5)
C(3)−C(4)−C(5)	128.1(13)	121.5(5)
C(3)−C(4)−C(11)	125.8(13)	124.1(5)
C(5)−C(4)−C(11)	106.0(12)	114.3(5)

double bond C(3)−C(4) corresponds to that (1.34 Å) of a normal ethylene group.[23] The two independent (DACH)Pt(FM) molecules depicted in Figure 2 show a dimeric interaction through the intermolecular hydrogen bonding, resulting in a Pt−Pt distance of 3.47(1) Å, within the sum of the van der Waals radii (3.60 Å).

For the (DACH)Pt(BHM), there are also two independent molecules in an asymmetric region of the triclinic unit cell. One of the molecular structures of (DACH)Pt(BHM) is shown in Figure 3, and selected bond distances and angles are listed in Table 4. The local geometry around the platinum atom is very similar to the structure of (DACH)Pt(FM) described above. The dihedral angle between two square planes of Pt(1), N(1), N(2), O(1), and O(3) and of C(1), C(2), C(3), C(4), C(5), and C(11) is about 80.8(2)°, and the planes of two phenyl rings of the BHM ligand are close to orthogonal (86.1(2)°). In the solid state two (DACH)Pt(BHM) molecules in centrosymmetric relation are held together by intermolecular N−H- -O hydrogen interactions (N···O distances, 3.02−3.03 Å). The Pt−Pt distance is 3.37(1) Å, within the sum of the van der Waals radii.

Multinuclear NMR Spectroscopy. ^{13}C NMR data of all the title complexes could be clearly assigned. Appearance of a single carboxylate ^{13}C chemical shift for the present complexes in the range of 171.7−171.8 ppm indicates that the bonding mode of the carboxylates is retained without dissociation in Me_2SO solution. The peak for C(9) in (DACH)Pt(FM) lies at 139.4 ppm, which is shifted 2.0 ppm upfield relative to that of the corresponding carbon of (DACH)Pt(BHM). Such a difference of the chemical shift seems to originate from the structural difference between the FM and BHM ligands in solution. Similar results were observed for the THPDMA analogs.

(23) Morrison, R. T.; Boyd, R. N. *Organic Chemistry*, 3rd ed.; Allyn and Bacon Inc.: Boston, MA, 1973; p 145.

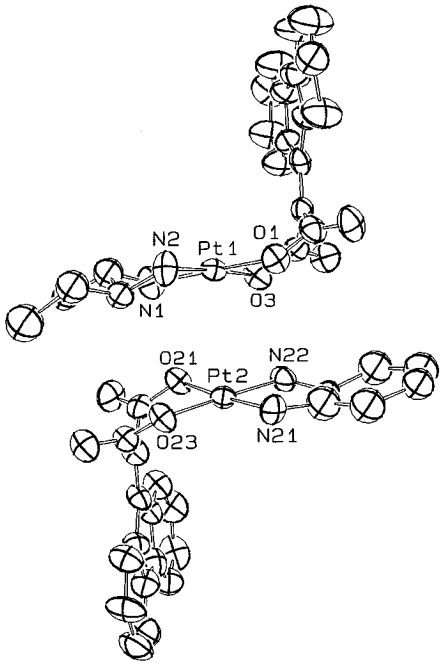

Figure 2. View showing the weak pairing of (DACH)Pt(FM) molecules within the unit cell. The separation between adjacent platinums is 3.47(1) Å, and the square plane around the platinum atom is essentially planar.

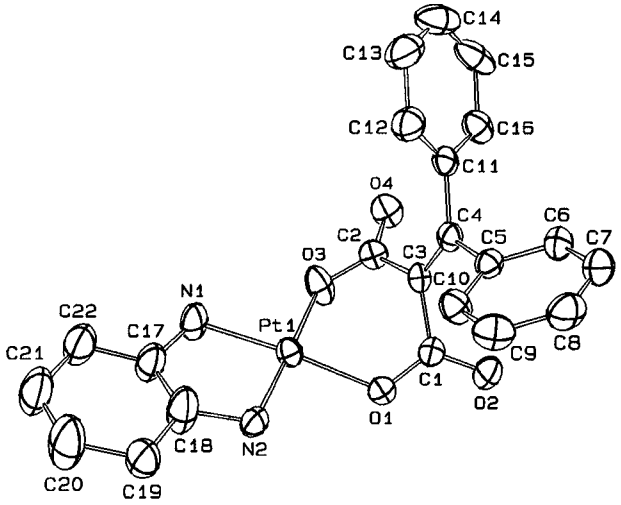

Figure 3. ORTEP drawing of (DACH)Pt(BHM) showing the atom-numbering scheme. The thermal ellipsoids are drawn at the 50% probability level.

The ^{195}Pt NMR spectra of the title complexes were measured in Me_2SO-d_6. Each spectrum of the present complexes exhibits only one ^{195}Pt resonance, reflecting the presence of one platinum species in the solution. Furthermore, the chemical shifts in the region −1844 to −1917 ppm are similar to those (−1930 to −1950 ppm) of (DACH)Pt(steroids), which are already elucidated as (*N*,*N*′-DACH)Pt(*O*,*O*′-chelated steroids).[4] The difference (44 ppm) between the ^{195}Pt chemical shifts of (THPDMA)-Pt(BHM) and (DACH)Pt(BHM) approximates to the difference (40 ppm) between those of (DACH)Pt(FM) and (THPDMA)-Pt(FM). The differences between the ^{195}Pt chemical shifts of (THPDMA)Pt(BHM) and (THPDMA)Pt(FM) and between those of (DACH)Pt(BHM) and (DACH)Pt(FM) are 33 and 29 ppm, respectively. Thus in the present platinum complexes, the variations of both amine and anionic carboxylate ligands affect significantly the platinum nuclear magnetic environment, even though the donor atoms and the local geometry of platinum atom are nearly identical.

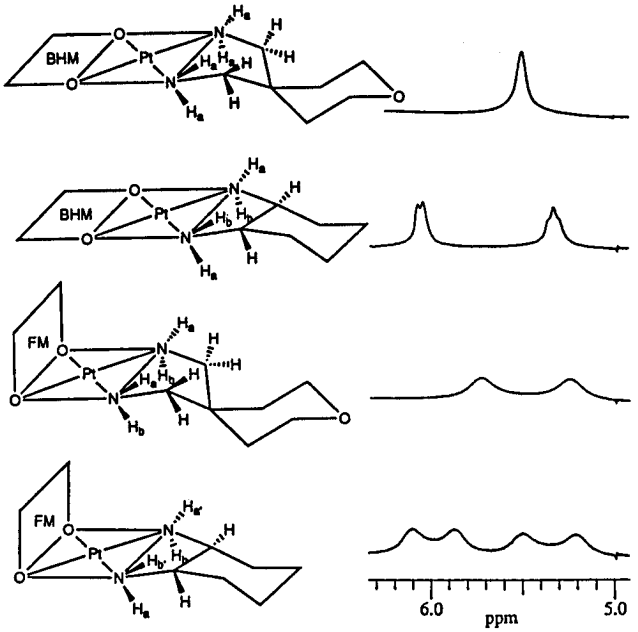

Figure 4. Molecular conformations and their amine ^{1}H NMR spectra in Me_2SO-d_6 solution at room temperature.

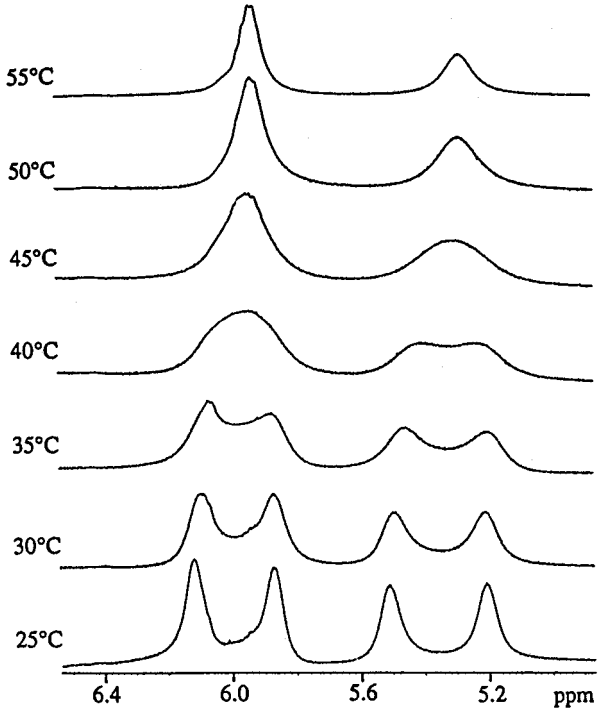

Figure 5. Variable-temperature amine ^{1}H NMR of (DACH)Pt(FM) in Me_2SO-d_6 (600 MHz).

^{1}H NMR spectral data of the present complexes are also consistent with the ^{195}Pt NMR data and the X-ray structures. In particular, the amine proton resonances appearing in the region 5.0−6.2 ppm are not equivalent as shown in Figure 4, indicating that each complex behaves characteristically at room temperature. The amine protons of (THPDMA)Pt(BHM) appear at 5.48 ppm as a singlet, whereas those of (THPDMA)Pt(FM) consist of two singlets at 5.23 and 5.72 ppm. While the amine proton peaks of (DACH)Pt(FM) are composed of four singlets at 5.21, 5.50, 5.87, and 6.10 ppm, those of (DACH)Pt(BHM) appear at 5.33 and 6.05 ppm as a triplet and a doublet, respectively. Both the triplet and doublet are each confirmed as a doublet of doublets by decoupling technique. The amine proton resonances of the complexes can be assigned assuming

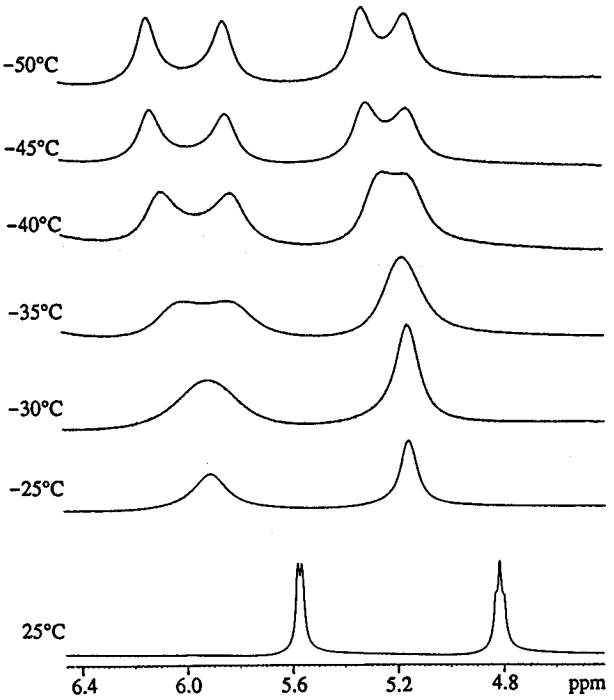

Figure 6. Variable-temperature amine ^{1}H NMR of (DACH)Pt(BHM) in dimethylformamide-d_7 (600 MHz).

Scheme 1

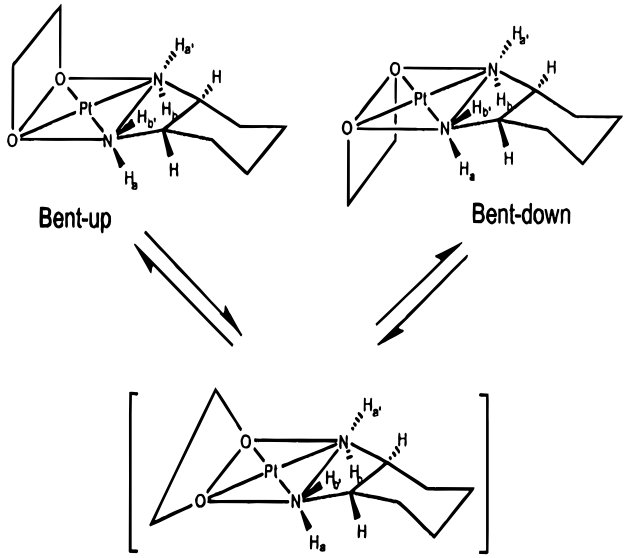

the molecular structures shown in the figure, where the BHM anionic ligand is represented to be coplanar with the platinum square plane, since it seems to become fluxional in solution at room temperature. However, the bent structure of the FM ligand seems to be retained even in solution at room temperature due to its inherent angle constraint. Thus even though the complexes have the same amine ligand, the resonances of the amine protons are greatly affected by the structure and behavior of the anionic carboxylate coligands FM and BHM, which are remote from the amine groups. Comparisons between the complexes of the same anionic ligands, that is, (THPDMA)Pt(BHM) and (DACH)-Pt(BHM), or (THPDMA)Pt(FM) and (DACH)Pt(FM), also disclose some structural aspects of α-carbon protons of THPDMA and DACH, where α-carbons next to the amine of THPDMA are primary and those of DACH are secondary.

The amine region of the proton spectra of (DACH)Pt(FM) exhibit a marked temperature dependence in the range 25−50 °C as shown in Figure 5. The molecule of (DACH)Pt(FM) is

fluxional in solution at above 45 °C. The room temperature spectrum shows four resonances at 5.21, 5.50, 5.87, and 6.10 ppm, consistent with the crystal structure of the complex. Warming the sample results in broadening of the resonance peaks with each pair coalescing at 40 and 45 °C, and further warming gives two resonances at 6.06 and 5.25 ppm, respectively, of nearly equal intensity. The process for the amine protons exchange is interpreted as reflecting an interconversion of the following equilibration shown in Scheme 1. In particular, observation of the two coalescing temperatures (T_c = 40 °C, $\Delta G^{\ddagger}$ = 14.7 kcal/mol; T_c = 45 °C, $\Delta G^{\ddagger}$ = 14.9 kcal/mol)[24] implies that the interconversion occurs through an unsymmetrical fluxional process as shown in Scheme 1. Thus, the amine region of the proton NMR of (DACH)Pt(FM) at elevated temperature approaches the room temperature spectrum of (THPDMA)Pt(FM). The variable temperature NMR spectra of (THPDMA)Pt(FM) in the same region also show interconversion between the two bent forms. The amine proton resonance is clearly observed at 5.23 and 5.72 ppm at room temperature, but as the sample temperature is increased, resonance peaks become broadened and coalesce at 50 °C with a free energy of activation $\Delta G^{\ddagger}$ = 15.0 kcal/mol. Above 50 °C a single resonance at the fast-exchange limit is observed at 5.48 ppm. Thus at elevated temperature the amine proton spectrum of (THPDMA)Pt(FM) approximates the room temperature spectrum of (THPDMA)Pt(BHM). Furthermore, variable temperature ^{1}H NMR of (DACH)Pt(BHM) was also monitored for the same proton region (Figure 6). Cooling the sample results in broadening of the two peaks, each being finally separated into two peaks, the first coalescing at −35 °C and the second at −40 °C. Thus at below −40 °C the amine proton of (DACH)-Pt(BHM) is in an environment similar to that of (DACH)Pt-(FM) at room temperature. Such a striking temperature-difference of coalescence between the two series of the FM and BHM complexes seems to be attributed to the presence or absence of the angle constraint of the anionic ligands in solution.

In conclusion, for the (diamine)platinum(II) complexes involving arylidene anionic ligands, a prominent molecular dynamics on the amine protons was observed due to the fluxional motion of the remote anionic ligands which depends on the temperature. More extensive studies on the nature of anionic ligands that may be concerted with the amine ligand behavior are necessary to help understand the biological activity and pharmacokinetics of platinum anticancer agents.

Acknowledgment. This research was supported financially by the Ministry of Science and Technology in Korea. We would like to thank Dr. Jongki Hong for the mass measurements.

Supporting Information Available: Tables giving details of X-ray data collection parameters, atomic coordinates, anisotropic thermal parameters, bond lengths and angles, hydrogen atom parameters, and least-square planes for 1 and 2 (22 pages). Ordering information is given on any current masthead page.

IC951011+

(24) $\Delta G^{\ddagger}$ values were calculated from $k_c = \pi\Delta\nu/\sqrt{2}$; $\Delta G^{\ddagger} = 2.3RT_c(10.32 + \log(T_c/K_c))$.